

This work was written as part of one of the author's official duties as an Employee of the United States Government and is therefore a work of the United States Government. In accordance with 17 U.S.C. 105, no copyright protection is available for such works under U.S. Law.

Public Domain Mark 1.0

<https://creativecommons.org/publicdomain/mark/1.0/>

Access to this work was provided by the University of Maryland, Baltimore County (UMBC) ScholarWorks@UMBC digital repository on the Maryland Shared Open Access (MD-SOAR) platform.

Please provide feedback

Please support the ScholarWorks@UMBC repository by emailing scholarworks-group@umbc.edu and telling us what having access to this work means to you and why it's important to you. Thank you.



LETTER

Recent global warming as confirmed by AIRS

OPEN ACCESS

RECEIVED
17 October 2018

REVISED
10 December 2018

ACCEPTED FOR PUBLICATION
10 January 2019

PUBLISHED
17 April 2019

Original content from this work may be used under the terms of the [Creative Commons Attribution 3.0 licence](#).

Any further distribution of this work must maintain attribution to the author(s) and the title of the work, journal citation and DOI.



J Susskind¹, G A Schmidt² , J N Lee^{1,3} and L Iredell^{1,4}

¹ NASA Goddard Space Flight Center, Greenbelt, MD, United States of America

² NASA Goddard Institute for Space Studies, New York, NY, United States of America

³ Joint Center for Earth Systems Technology, University of Maryland Baltimore County, Baltimore, MD, United States of America

⁴ ADNET/NASA, Code 610.2 Greenbelt, MD, United States of America

E-mail: Joel.Susskind-1@nasa.gov

Keywords: global surface temperature, recent warming, AIRS, GISTEMP

Abstract

This paper presents Atmospheric Infra-Red Sounder (AIRS) surface skin temperature anomalies for the period 2003 through 2017, and compares them to station-based analyses of surface air temperature anomalies (principally the Goddard Institute for Space Studies Surface Temperature Analysis (GISTEMP)). The AIRS instrument flies on EOS Aqua, which was launched in 2002 and became stable in September 2002. AIRS surface temperatures are completely satellite-based and are totally independent of any surface-based measurements. We show in this paper that satellite-based surface temperatures can serve as an important validation of surface-based estimates and help to improve surface-based data sets in a way that can be extended back many decades to further scientific research. AIRS surface temperatures have better spatial coverage than those of GISTEMP, though at the global annual scale the two data sets are highly coherent. As in the surface-based analyses, 2016 was the warmest year yet.

1. Introduction

Surface temperature change and variability is a critical component of the Earth's climate. Instrumental weather station data and ocean sea surface measurements are available back to the 19th century with reasonable global coverage, allowing for well-constrained estimates of global and regional surface temperature change since then (Hansen *et al* 2010, Morice *et al* 2012, Vose *et al* 2012, Rohde *et al* 2013). Despite the overall trends being 'unequivocal' (IPCC 2013) there has been intense interest in the details of how these estimates are constructed and how known imperfections in the raw data (due to station moves, gaps, instrument and practice changes, urban heat island effects etc) are handled (see Karl *et al* 2015). This paper does not attempt to address the reasons why global mean surface temperatures have been warming lately. Rather, the purpose is to demonstrate that this previously reported result of recent global warming as depicted in many ground based data sets is confirmed in the totally independent satellite-based Atmospheric Infra-Red Sounder (AIRS) data set.

While intensive studies are still needed to estimate the uncertainties of satellite observations in global scale,

systematic observations with consistent temporal and spatial coverage from satellites still can be a crucial complement to the surface-based estimates to better assess surface temperature changes (Merchant *et al* 2013, Veal *et al* 2013, Merchant *et al* 2017). Number of algorithms are developed to retrieve surface temperatures from an Along Track Scanning Radiometer 2 (ATSR-2) infra-red (IR) channels, but no single algorithm is valid to produce surface temperature over different surfaces (Sobrino *et al* 2004 and reference therein). The temperature sounding microwave (MW) radiometers, microwave sounding unit (MSU) and advanced MSU (AMSU) have provided additional related measures of climate change (Mears and Wentz 2017, Spencer *et al* 2017), but reflect lower-to-mid tropospheric bulk temperatures and so have not served as a direct validation of the *in situ* surface temperature data set products. Satellite-based temperature measurements from multiple platforms also required significant efforts for a number of adjustments to account for calibration and drift of local measurement time, to be assembled into a single long-term data record (Mears and Wentz 2017 and references therein). MW imagers such as AMSR-E (Gentemann 2014) and AMSR-2 (Gentemann and Hilburn 2015) that have

polarized channels near 7, 11, 19, and 37 GHz allow retrievals of SST, emissivity, and atmospheric emission. MW imagers are primarily sensitive to the surface skin temperature and surface emissivity, and are less sensitive to changes in clouds and water vapor than are IR instruments such as Moderate Resolution Imaging Spectroradiometer (MODIS), and especially AIRS because AIRS determines surface temperature and emissivity in the 3.7 μm region. The observations from MW channels are more suitable than from IR observations over ocean because they do not have the inherent sampling biases from cloud contamination. However, MW detection of surface temperatures are less useful than over ocean because of uncertainties in surface emissivity.

The IR MODIS generated surface skin temperature data sets, but used separate algorithms over land (Hulley and Hook 2017), ice (Hall *et al* 2004), and ocean (Brown and Minnett 1999). These limitations do not apply to the AIRS surface temperature data record which uses identical methodology to determine surface skin temperatures and surface emissivity over all surfaces. AIRS data covers pole to pole (90°S–90°N) on a 1° latitude by 1° longitude spatial grid with no spatial gaps, with daily observations from ascending and descending orbits, as described in the following section.

2. Data and methods

2.1. Data

2.1.1. AIRS surface skin temperature

AIRS is a high spectral resolution IR sounder that was launched on Earth Observing System (EOS) Aqua in 2002. The AIRS Science Team Version-6 ‘AIRS Only (AO)’ data set is the current official AIRS Science Team data set (Susskind *et al* 2014). The AIRS data set begins in September 2002, when the AIRS instrument became thermally stable, and, at the time of this writing, extends through November 2018. There have been no changes made to the data used to generate AIRS data products, nor to the scientific methodology used to analyze the data. The AIRS data set contains many monthly mean geophysical parameters in addition to surface skin temperature. More details about AIRS and how quality controlled geophysical parameters are determined from AIRS observations are given in [appendix](#).

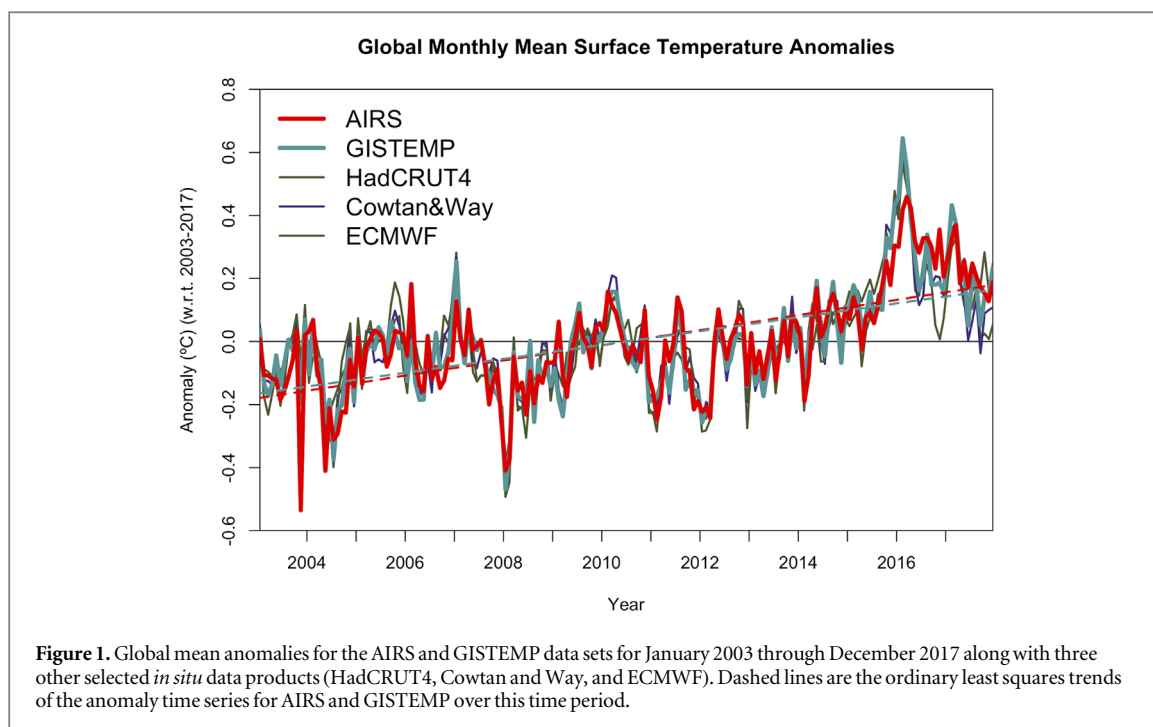
AIRS monthly mean products are generated globally on a 1° latitude by 1° longitude spatial grid with no spatial gaps. Separate monthly mean products are generated for EOS Aqua ascending orbits AIRS_{PM} (nominally at 1:30 PM local time) and for descending orbits AIRS_{AM} (nominally at 1:30 AM local time). The results shown in this paper use the average of the AIRS_{PM} and AIRS_{AM} data sets. The EOS Aqua orbit is stabilized by periodic orbit adjustments and consequently there has been no drift in the EOS Aqua orbit over the time period under study.

2.1.2. In-situ and reanalysis-based surface temperature products

There are a number of official analyses of surface temperature anomalies from Goddard Institute for Space Studies Surface Temperature Analysis (GISTEMP) (Hansen *et al* 2010), NOAA NCEI (Vose *et al* 2012), the Hadley Centre/Climatic Research Unit (Morice *et al* 2012), and the Japanese Meteorological Agency (Ishihara 2006). Additionally, at least two institutionally independent efforts have recently emerged that apply new methodologies and/or use expanded data sets (Rohde *et al* 2013, Cowtan and Way 2014a).

GISTEMP is a well-used example of these products and makes use of *in situ* surface measurements over land, assembled from publicly available surface air temperature data acquired by about 6300 meteorological stations around the world, an analysis of ship- and buoy-based sea surface temperatures (Huang *et al* 2017), and Antarctic weather stations. The spatial distribution of stations is sufficient from 1880 onwards to produce a reasonable estimate of the global anomalies, although coverage is sparse in some areas, especially over the Arctic and Antarctic, as well as parts of Africa and South America. The GISTEMP analysis uses anomaly data sampled on an equal area grid and reports anomalies for each month from a 1951–1980 climatology. Monthly data are presented on a 2° latitude by 2° longitude spatial grid. The other analyses of surface station data differ in the treatment of urban heating effects, interpolation across data poor areas, homogenization treatments of the data to remove non-climatic artifacts, and ocean temperature products but are very similar in terms of trends and annual anomalies (Sánchez-Lugo *et al* 2018). Notably, the HadCRUT4 and NCEI analyses do not extrapolate to data poor areas (such as the Arctic). Cowtan and Way’s analysis uses the same base data as HadCRUT4 but uses kriging to extend the data to be spatially complete (Cowtan and Way 2014a) and we use this in comparisons below. Coverage biases, particularly in the earlier decades, may contribute to an overall underestimate of the long-term trends (Richardson *et al* 2016). Output data from re-analyses can be used to independently characterize the surface temperature changes once inhomogeneities in data processing and inputs have been corrected for. We use a product based on the European Centre for Medium-Range Weather Forecasts (ECMWF) Interim Analysis. In all of these records, most of the Earth’s warming since 1880 occurred in the past 35 years, with 16 of the 17 warmest years on record occurring since 2001 (NASA Public Affairs 2018). Recently Way *et al* (2017) suggested that warming in Northern Canada is underestimated in surface-based data sets due to a systematic cold bias originating from the automated homogenization algorithm of the station data processing. Cowtan and Way (2014a, 2014b) also suggested that *in situ* measured surface temperature data may result in an underestimation of recent Arctic warming.

The AIRS data reflects skin temperature at the very surface (top mm) of the ocean, land, and snow/ice



covered regions (Susskind *et al* 2003, 2006, 2011). The surface-based products are a blend of 2 m surface air data anomalies over land, and bulk sea surface temperature anomalies in the ocean (top 5 m). The mean values from each class of product are therefore not expected to match. For anomaly data, comparisons with climate model output suggest that there is a small bias (~ 0.02 °C/decade) between this form of blended product and the ‘true’ global mean surface air temperature anomaly (Cowtan *et al* 2015). The products also differ in spatial coverage. AIRS retrievals are almost complete, producing data up to both poles (though gaps and uncertainties increase in areas of high cloud cover). GISTEMP, and the Cowtan and Way (C&W) products use different methods to fill in data near the poles and in other data sparse regions, while the Hadley Center/Climatic Research Unit (HadCRUT4), NOAA NCEI, and the JMA publish averages only over the directly sampled regions. Comparisons with reanalysis products suggest that the surface-based products that do extrapolate across the pole have less bias with respect to the true global mean (Simmons *et al* 2016).

We constructed monthly grid point climatologies for each calendar month and for each product by averaging the monthly values over the 15-year period 2003 through 2017, with anomalies for a given month, in a given year, defined as the difference of the grid point value for that month from its monthly climatology.

3. Results

3.1. Monthly mean anomalies and spatial trends

Figure 1 shows monthly global mean anomalies for each month from January 2003 through December

2017 from AIRS, GISTEMP and three other selected products. Also shown in figure 1 are the slopes of the linear least squares fits of the AIRS and GISTEMP anomaly time series. The agreement of the global mean monthly anomalies of the AIRS and GISTEMP time series is very good, with a temporal correlation of 0.92, excluding November 2003 during which AIRS was shut down for a substantial part of the month. AIRS data show a slightly greater short term warming trend than found in GISTEMP or the other products (table 1).

The trend lines shown in figure 1 are representative of changes in area-weighted temperatures averaged over the whole globe. However, the warming is not spatially homogeneous. Figure 2 shows 15-year zonal mean trends as a function of latitude for AIRS and GISTEMP. Both AIRS and GISTEMP show considerable latitudinal structure in zonal mean trends. Both show considerable warming over the last 15 years poleward of 65°N , and also warming, through less so, poleward of 80°S . GISTEMP shows less warming than AIRS at high latitudes in the Northern Hemisphere. The latitudinal region between 68°S and 58°S has actually cooled over this time period, and GISTEMP shows less cooling than AIRS there. Most of the rest of the globe has been marked by more modest warming trends. As in figure 1, the AIRS global mean short term trend is slightly more positive than that of GISTEMP. This is primarily a result of GISTEMP having weaker Northern Hemispheric polar warming trends than does AIRS.

Figures 3(a) and (b) show spatial plots of 15-year trends of AIRS and GISTEMP surface temperature anomalies. The area-weighted global mean 15 year trends are 0.24 °C/decade and 0.22 °C/decade respectively.

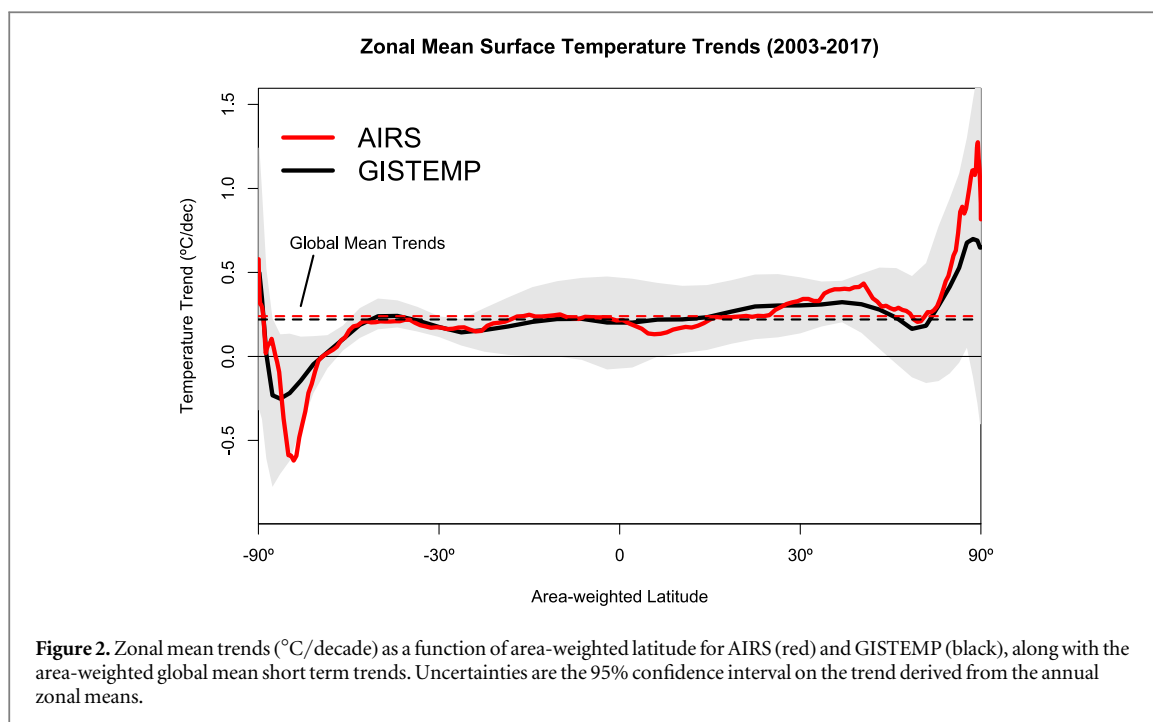


Table 1. Trends and cross-product correlations of the global mean surface temperature products over 2003–2107. Trend uncertainties are 95% confidence intervals (2.16 standard deviations from the linear fits, based on the Students' t-test with 14 degrees of freedom) from annual data. Correlations are either annual, or monthly (excluding November 2003 from AIRS).

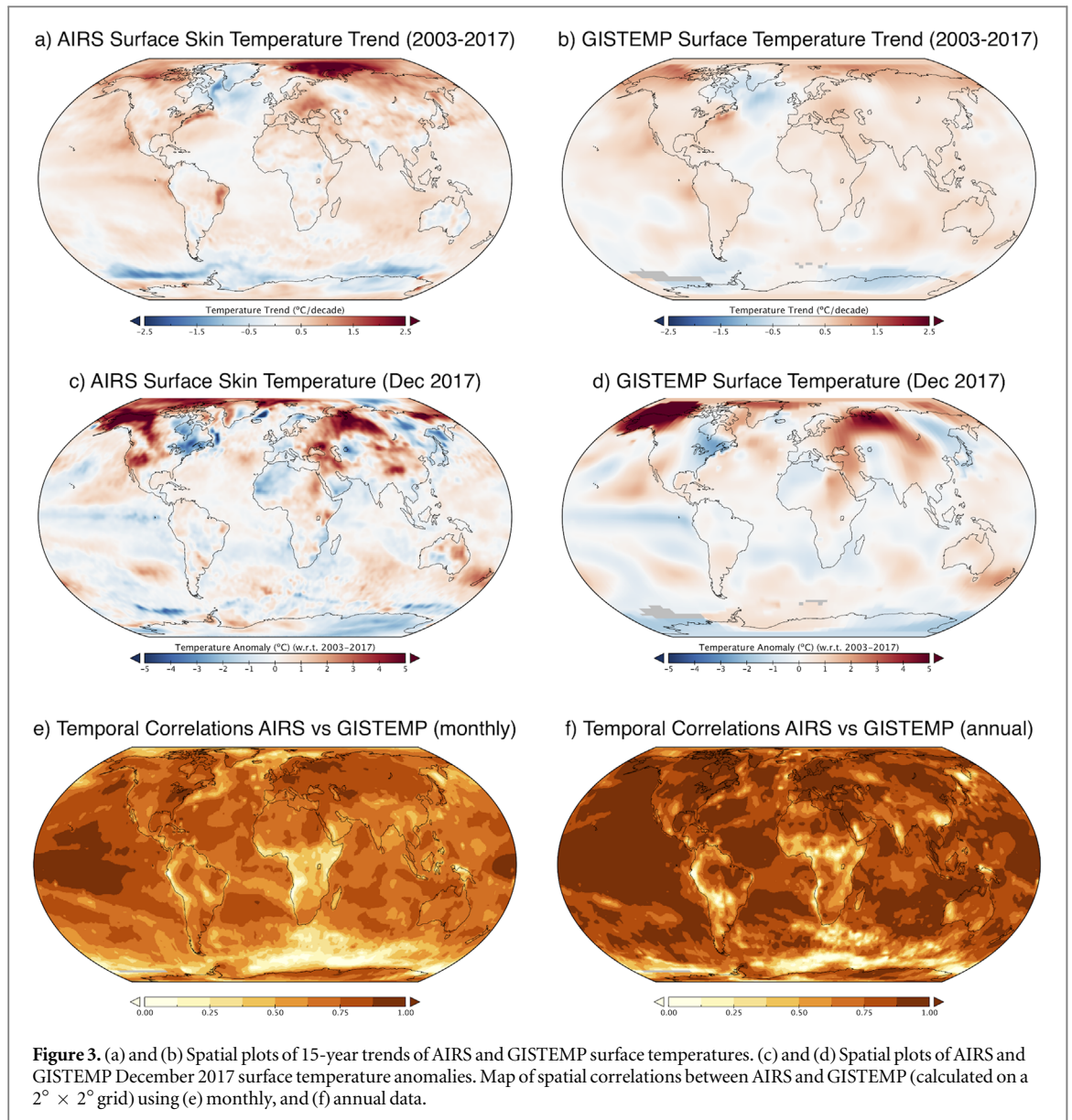
	Trend (2003–2017) ($^{\circ}\text{C}/\text{decade}$)	Correlations of global mean anomalies (Ann/Mon) (2003–2017)			
		GISTEMP	HadCRUT4	C&W	ECMWF
AIRS	0.24 ± 0.12	0.98/0.92	0.93/0.84	0.97/0.89	0.96/0.90
GISTEMP	0.22 ± 0.13		0.97/0.92	0.99/0.95	0.97/0.92
HadCRUT4	0.17 ± 0.13			0.98/0.94	0.94/0.88
C&W	0.19 ± 0.12				0.96/0.94
ECMWF	0.20 ± 0.16				

Temperature trends have considerable longitudinal structure at a given latitude. The spatial distributions of AIRS and GISTEMP trends are very similar, except that the AIRS features are sharper and larger than those of GISTEMP as a result of both higher spatial resolution and better spatial coverage. The area-weighted spatial correlation of figures 3(a) and (b) at the GISTEMP resolution is 0.74.

While temperatures poleward of 60°N have warmed considerably, both data sets show Greenland, as well as the ocean south of it, have cooled over the last 15 years. This cooling over Greenland is a relatively recent phenomenon, however. McGrath *et al* (2013) showed that previous *in situ* measurements at Summit, Greenland suggest that Greenland's annual mean near-surface air temperature increased by $0.9^{\circ}\text{C} \pm 0.1^{\circ}\text{C}/\text{decade}$ during 1982–2011, and that the local increase over Greenland was six times larger than the warming rate of the global mean temperature during that time period. Both AIRS and GISTEMP show that there has

also been cooling in the Southern Oceans during the last 15 years.

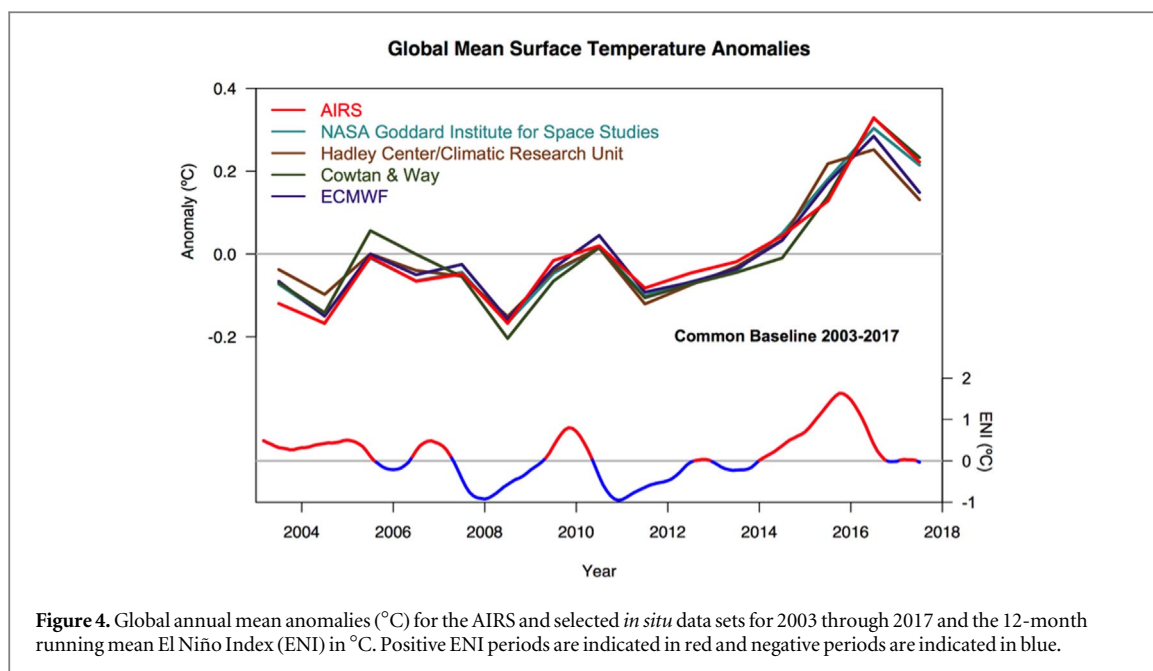
AIRS surface temperature trends indicate that the greatest warming in the last 15 years occurred over the Barents and Kara Seas with trends larger than $2.5^{\circ}\text{C}/\text{decade}$. The positive AIRS Arctic warming trend poleward of 60°N is consistent with Cullather *et al* (2016), who showed that the MERRA-2 reanalysis surface temperature recorded the warmest winter season over the Arctic in the observational record during the winter of 2016 (December 2015–February 2016). The temperature trends shown in figures 3(a) and (b) should not be necessarily taken to be indicative of the true long-term changes. For example, AIRS shows a short term 'El Niño trend' over the 15-year time period under study, and GISTEMP show a similar, but broader and weaker pattern. This is mainly a result of an El Niño event which took place off the west coast of South America in 2015 and 2016. Predictions of long-term warming in the El Niño region are quite



uncertain and subject to a lot of natural variability (Keupp *et al* 2017).

Figures 3(c) and (d) show AIRS and GISTEMP temperature anomalies for Dec 2017. Agreement between both sets of temperature anomalies is again extremely close, given the differences in spatial resolution and spatial sampling, with a spatial correlation of 0.74. The range of area-weighted spatial correlations over all months is 0.58 ± 0.1 (1 sigma) with maximum of 0.83 in November 2016 and minima of 0.13 in Nov 2003. The AIRS monthly mean data was affected by the solar proton event during Nov 2003 and the instrument did not collect the data for the first two weeks of the month. Depictions of AIRS single day surface temperature spatial coverages in Northern Hemisphere Winter and Northern Hemisphere Summer are given in the [appendix](#). AIRS single day spatial coverage over land is almost complete with the exception of orbit gaps at low latitudes which rotate around the Earth with an 8 day repeat cycle.

The December 2017 anomalies feature far more internal variability than the long-term trends. AIRS and GISTEMP both show large positive global mean anomalies for December 2017, with values of 0.19°C and 0.23°C respectively, despite the significant cold anomalies that took place in the northeastern United States and eastern Canada, as clearly depicted in both data sets. December 2017 also features a minor La Niña event that started in 2017. As shown in the next section, La Niña time periods typically correspond to local minima in annual mean surface temperature anomalies, and El Niño time periods correspond to local maxima. Figure 3(d) demonstrates a limitation of the GISTEMP data set in that the data coverage is sparse near the poles. This is evidenced by the relative lack of longitudinal variation poleward of 85°N , where GISTEMP is extrapolating over sea ice covered areas while AIRS is seeing longitudinal changes in skin temperature directly.



The maps of temporal correlations in figures 3(e) and (f) give insight into where the AIRS and GISTEMP products differ most—mainly the Southern Ocean, sub-Saharan Africa, and areas of high topography. This mainly mirrors regions in which there are coverage issues in the GISTEMP product. There is no indication of issues with areas that are heavily cloud covered, suggesting that the cloud clearing algorithms in AIRS are working well.

3.2. Global annual mean anomalies

Figure 4 shows global annual mean surface temperature anomalies for the AIRS and four surface-based data sets for 15 years 2003 through 2017. There is excellent agreement between all sets of annual mean anomalies. In particular, all five data sets show an increase in temperature, with 2016 being the warmest year, 2017 the second warmest year, and 2015 the third warmest year over the 15 years under study.

Figure 4 also shows the 12-month running mean of an El Niño Index (ENI) defined as the average of monthly mean grid point point SST anomalies using data over the combined Niño 4 and Niño 3 areas. We use the average anomaly over these two areas because while most El Niño/La Niña activity early in the time period under study took place in the NOAA Niño 4 region, El Niño/La Niña activity toward the end of the time period took place in the NOAA Niño 3 region off the west coast of South America.

As is well known, figure 4 demonstrates that local maxima in annual mean temperatures tend to occur in years that start with positive ENI (2003, 2005, 2007, 2010, 2015, 2016), and local minima tend to occur in years that have negative ENI (2006, 2008, 2011, 2017). 2017 started off with neutral ENI conditions, and developed mild La Niña conditions by the end of the year keeping the year relatively cool with respect to the

record years set previously. ENI in December/January explains about 62% (AIRS) or 70% (GISTEMP) of the residual variance in the following year's annual mean temperature anomaly.

The biggest difference between annual mean AIRS anomalies and those of GISTEMP and the other data sets occurs in 2003, which is the year that contained the anomalous AIRS month of November 2003, during which some AIRS data was missing. The most significant point of figure 4 is the strong coherence among the independent data sets both in the inter-annual variance and trends, including the record-breaking warmth in the later years.

Table 1 quantifies the 15-year trends (°C/decade) and inter-correlations of each data set, computed using the annual mean and monthly mean anomalies. All data sets show a highly significant warming trend of ~ 0.2 °C/decade over this time period. The AIRS warming trend is slightly higher than that of GISTEMP and the other data sets. There is no significant auto-correlation in the residuals from the linear trend on annual data, and so the trend uncertainties given are simply those from the ordinary least squares calculation. Trends in the non-spatially complete HadCRUT4 data set are the smallest of the 5 products. The AIRS anomaly time series strongly matches the independent GISTEMP anomaly time series very well in terms of trends and correlations in time ($r = 0.98/0.92$ using annual/monthly data). This is slightly higher than the correlation of AIRS anomalies with those of any of the other data products, but not significantly so.

4. Conclusions

The GISTEMP data set, and the totally independent satellite-based AIRS surface skin temperature data set,

are very consistent with each other over the past 15 years. Both data sets demonstrate that the Earth's surface has been warming globally over this time period, and that 2016, 2017, and 2015 have been the warmest years in the instrumental record, in that order. In addition to being an independent data set, AIRS products complement those of GISTEMP because they are at a higher spatial resolution than those of GISTEMP and have more complete spatial coverage, despite a shorter record. Differences in the products (and lower temporal correlations) mostly reflect areas without much directly observed station data (the Arctic, Southern Ocean, sub-Saharan Africa) suggesting that the fault lies in the station-based products rather than with the AIRS data. Notably, surface-based data sets may be underestimating the changes in the Arctic.

The characteristics of the Earth's climate change continually. Complementary satellite-based surface temperature analyses serve as an important validation of surface-based estimates, and they may point the way to make improvements in surface-based products that can perhaps be extended back many decades.

Acknowledgments

This work is supported by NASA Terra-Aqua Science Program (NNH13ZDA001N-TERAQ) and the NASA Modeling, Analysis and Prediction program. AIRS monthly mean products are obtained from https://acdsc.gesdisc.eosdis.nasa.gov/data/Aqua_AIRS_Level3/AIRS3STM.006/. GISTEMP data are obtained from <https://data.giss.nasa.gov/gistemp/>. ECMWF data were downloaded from <https://climate.copernicus.eu/resources/data-analysis/average-surface-air-temperature-analysis>. ENSO indices are taken from <http://cpc.ncep.noaa.gov/data/indices/sstoi.indices>. We thank the anonymous reviewers, whose comments and suggestions greatly improved the manuscript.

Appendix A. Quality control (QC) of AIRS surface skin temperatures (T_s)

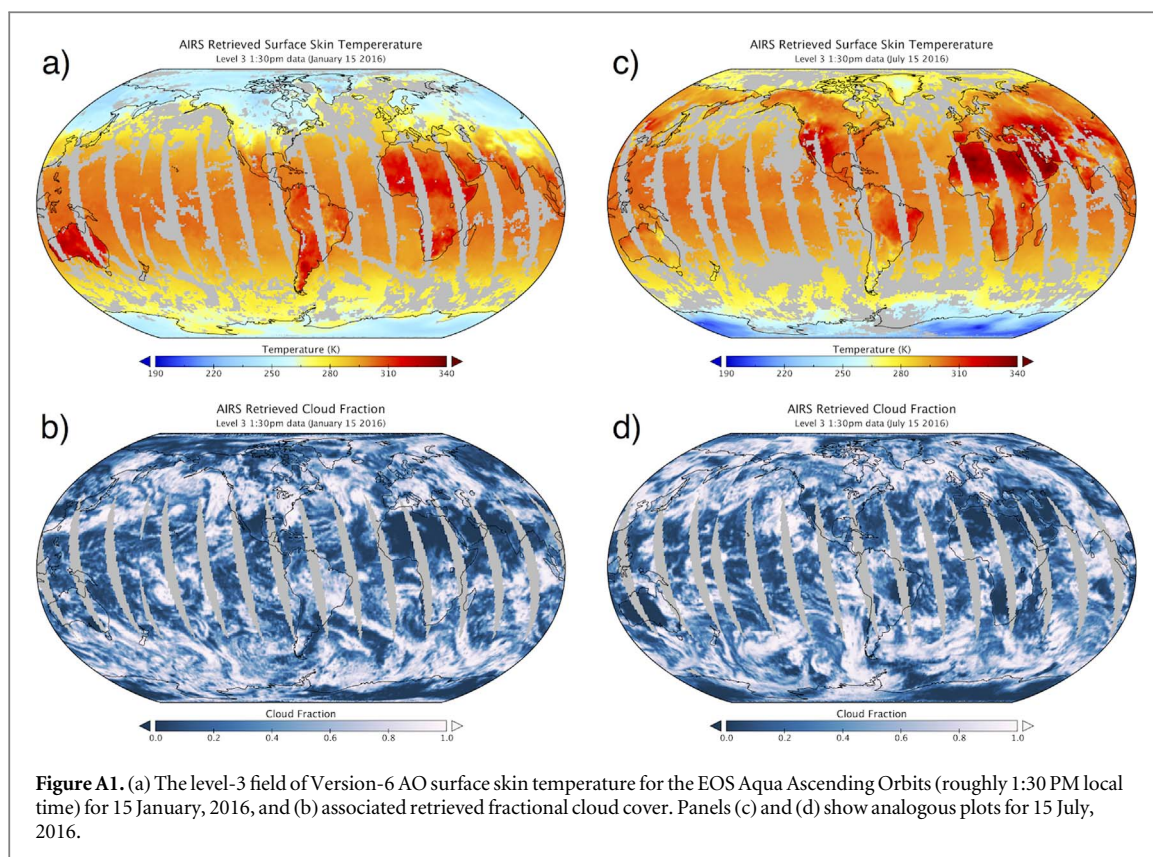
A1. Overview

The AIRS is a high spectral resolution IR sounder that was launched in May 2002 on EOS Aqua in a stable sun-synchronous orbit that observes the Earth twice daily, at roughly 1:30 AM and 1:30 PM local times. AIRS was accompanied by the AMSU (AMSU)-A to form a next-generation polar-orbiting IR and MW atmospheric-sounding system. There is a 3×3 array of AIRS fields of view (FOVs), with a spatial resolution of $13 \text{ km} \times 13 \text{ km}$ at nadir, within a single AMSU-A footprint, which is $45 \text{ km} \times 45 \text{ km}$ at nadir. With the exception of cloud parameters, a single AIRS retrieval is performed on a field of regard (FOR) basis, containing a 3×3 grouping of AIRS FOVs. The current operational AIRS Science Team retrieval algorithm

(Susskind *et al* 2014) is AIRS Version-6 AO, which uses AIRS observations, but does not use AMSU observations in any way. AIRS observations had been analyzed in parallel in both Version-6 AIRS/AMSU and Version-6 AO modes until some important AMSU channels died in September 2017, after which AIRS data was, and still is, analyzed only in the AO mode. Results using Version-6 AIRS/AMSU and Version-6 AO are similar to each other in the overlap period when both modes were being processed simultaneously. The results shown in this paper are monthly mean values of AIRS gridded level-3 1:30 AM/PM averages of T_s taken from the operational AIRS Version-6 level-3 AO data set. Both AIRS Version-6 data sets begin in September 2002 when the AIRS instrument became stable. AIRS level-3 products are presented on a $1^\circ \times 1^\circ$ latitude–longitude spatial grid, and extend from pole to pole. AIRS values of T_s represent the temperature of roughly the top mm of the solid earth.

Version-6 AO retrievals of all geophysical parameters from AIRS observations are physically based and do not use any information other than AIRS observations, with the exception of a forecasted surface pressure p_s , which is needed as a boundary condition when computing AIRS channel i radiances expected for the FOR state X . $R_i(X)$ is computed using a Radiative Transfer Model. The retrieved state for the FOR is the geophysical state for which the ensemble $R_i(X)$ best matches, in a weighted RMS sense, the set of channel clear column radiances R_i' for the subset of AIRS channels used to retrieve the appropriate geophysical parameters, which are a subset of the complete state X . R_i' are derived quantities, generated on a FOR basis, that represent the radiances that AIRS channel i 'would have seen' if the FOR were completely clear.

AIRS Version-6 retrieval methodology is described in detail in Susskind *et al* (2014), and the references therein, especially Susskind *et al* (2011). The retrieval process starts with a neural net initial guess X^0 for the FOR, from which initial values of AIRS clear column radiances are determined. AIRS channel clear column radiances are then used to sequentially determine: (1) surface skin temperature T_s , along with surface spectral emissivity and, during the day, surface bidirectional reflectance of solar radiation; (2) atmospheric temperature profile $T(p)$, including surface air temperature $T(p_s)$; (3) atmospheric moisture profile; (4) atmospheric ozone profile; (5) atmospheric CO profile; and (6) atmospheric CH_4 profile. These steps are done sequentially, solving only for the variables to be determined in each retrieval step using the appropriate set of channels for that step, and using previously determined variables as fixed but with an appropriate uncertainty attached to them, which is accounted for in a channel-noise covariance matrix. Steps 1–6 are ordered so as to allow for selection of channels in each step which are primarily sensitive to



variables to be determined in that step or determined in a previous step, and are relatively insensitive to other parameters. $T(p)$ is determined in the step after T_s is determined, and uses a different set of channels in the retrieval process. A cloud parameter retrieval is performed after the final surface and atmospheric state has been determined by finding cloud parameters for which the computed channel cloudy radiances, including both the cloud parameters and other retrieved parameters, is most consistent with the observed radiances for a subset of channels. Cloud parameters are retrieved on a FOV basis and are always generated as long as AIRS observations are present.

A2. Surface skin temperature QC

Susskind *et al* (2014) describes the QC procedures used for all geophysical parameters in AIRS Version-6 and AIRS Version-6 AO retrievals. QC flags are generated for all geophysical parameters X_j , and are based on thresholds of error estimates for each parameter j contained in X_j . Each retrieved geophysical parameter for a FOR is given a QC flag which is equal to 0 (highest quality), 1 (good quality) or 2 (poor quality) which depend both on the error estimate for that geophysical parameter and parameter dependent thresholds. Gridded level-3 products for parameter j include only those cases with QC Flags 0 or 1. Cases with QC flags = 2 are excluded from the generation of the level-3 product for that geophysical parameter. QC thresholds for oceanic values of T_s are considerably tighter than those for T_s over land or frozen ocean,

both because ocean surface skin temperatures are already known very well based on ship measurements, and also because ocean surface skin temperatures change very slowly in space and time. Susskind *et al* (2014) show that Version-6 AO oceanic surface skin temperatures between 50°S and 50°N , with $QC = 0$ or 1, have an acceptance yield of about 50% with a bias compared to collocated ECMWF ‘truth’ of -0.34 K and a spatial standard deviation of 0.95 K compared to ECMWF values. It must be remembered that ECMWF oceanic surface skin temperatures are reasonably accurate in general, but are not perfect. It is possible that QC’d AIRS retrieved values of T_s over ocean are actually more accurate than those of ECMWF, especially in regions far from where ship measurements are made. QC thresholds for T_s over land and frozen ocean are considerably larger than those over non-frozen ocean, both because T_s is not well known from other sources over land and ice, and also because land values of T_s change rapidly in space and time. For this reason, it is more important to maintain the highest spatial coverage of AIRS retrieved values of T_s over land and ice, provided they have reasonable error estimates.

A3. Sample level-3 single day fields of T_s and cloud cover

Sample ascending mode single day gridded $1^\circ \times 1^\circ$ level-3 fields of AIRS Version-6 AO surface skin temperature and cloud cover in two different seasons are shown in figure A1. These results are indicative of the spatial sampling and spatial coverage contained in

single day AIRS surface skin temperatures in Northern Hemisphere winter and summer respectively. Figures A1(b) and (d) show level-3 cloud fields for a day in January and a day in July. Cloud products are always generated provided valid AIRS radiances exist. These figures clearly depict gaps between the different orbits of EOS Aqua, which are largest near the equator. AIRS scans from side to side as it flies along the orbit, but the swath width is smaller than the separation of the orbits at low latitudes. 85% of the Earth's area has coverage in the January cloud field, and 84% of the Earth is covered in the July cloud field. The orbits move from day to day, with an eight-day repeat cycle. The existence of these moving gaps will influence monthly mean products and their inter-annual differences to some extent. The results shown in this paper indicate that this is not a big concern regarding AIRS products on the monthly mean time scale.

Figures A1(a) and (c) show spatial plots of level-3 fields of surface skin temperatures for 15 January and 15 July respectively. Grid points containing no cloud data also contain no surface skin temperature data, because a lack of cloud data means there were no AIRS observations in that grid box. In January, 69% of the Earth has skin temperature coverage, which is 81% of the area observed by AIRS, and, in July, 63% of the Earth contains skin temperatures, corresponding to 75% of the grid points observed by AIRS. Most of the grid points observed by AIRS, in which surface skin temperatures are missing, occur over ocean, in locations containing large amounts of cloud cover. For the most part, cloud cover moves from day to day, and this does not significantly degrade the monthly mean ocean skin temperature product. Land and ice surface skin temperature coverage on a daily basis is almost complete. This is a result of the use of looser QC thresholds over land and ice than over ocean because of the need to maintain good spatial coverage over these areas.

Grid points containing no data are shown in gray in the figures. Warm temperatures in panels (a) and (c) are in shades of yellow and red, and cold temperatures are in shades of blue. Very cloudy grid points are indicated in white in panels (b) and (d), and very clear grid points are indicated in dark blue.

Estimate of the uncertainty in the satellite measurements of surface temperature due to inconsistent temporal and spatial sampling is a challenging task (Mears *et al* 2011). The sampling bias in AIRS monthly mean product can be separated into two components; temporal and instrument biases. The temporal bias is caused by two times of observation from Aqua ascending and descending orbit in a given day and location. The instrumental sampling biases are uncertainties caused by scenes that prevent successful retrievals of surface temperature due to orbit gaps and overcast clouds, as mentioned above. The regional instrumental sampling bias of surface temperature can be up to ± 2 °C. The temporal sampling biases are generally smaller than the instrumental sampling biases except

in regions with large diurnal variations where it can be up to ± 2 °C over desert area (Hearty *et al* 2014).

ORCID iDs

G A Schmidt  <https://orcid.org/0000-0002-2258-0486>

J N Lee  <https://orcid.org/0000-0001-9814-9855>

L Iredell  <https://orcid.org/0000-0001-7224-8687>

References

- Brown O B and Minnett P J 1999 MODIS infrared sea surface temperature algorithm theoretical basis document, version 2.0 http://modis.gsfc.nasa.gov/data/atbd/atbd_mod25.pdf (Accessed: 3 December 2018)
- Cowtan K, Hausfather Z, Hawkins E, Jacobs P, Mann M E, Miller S K, Steinman B A, Stolpe M B and Way R G 2015 Robust comparison of climate models with observations using blended land air and ocean sea surface temperatures *Geophys. Res. Lett.* **42** 6526–34
- Cowtan K and Way R G 2014a Coverage bias in the HadCRUT4 temperature series and its impact on recent temperature trends *Q. J. R. Meteorol. Soc.* **140** 1935–44
- Cowtan K and Way R G 2014b Update to 'Coverage bias in the HadCRUT4 temperature series and its impact on recent temperature trends' *Reconciling Glob. Temp. Ser.* **4** 27
- Cullather R I, Lim Y-K, Boisvert L N, Brucker L, Lee J N and Nowicki S M J 2016 Analysis of the warmest Arctic winter, 2015–2016 *Geophys. Res. Lett.* **43** 808–10
- Gentemann C L 2014 Three way validation of MODIS and AMSR-E sea surface temperatures *J. Geophys. Res. Oceans* **118** 2583–98
- Gentemann C L and Hilburn K A 2015 *In situ* validation of sea surface temperatures from the GCOM-W1 AMSR2 RSS calibrated brightness temperature *J. Geophys. Res.* **120** 3567–85
- Hall D K, Key J, Casey K A, Riggs G A and Cavalieri D J 2004 Sea ice surface temperature product from the Moderate Resolution Imaging Spectroradiometer (MODIS) *IEEE Trans. Geosci. Remote Sens.* **42** 1076–87
- Hansen J, Ruedy R, Sato M and Lo K 2010 Global surface temperature change *Rev. Geophys.* **48** RG4004
- Hearty T J, Savtchenko A, Tian B, Fetzer E, Yung Y L, Theobald M, Vollmer B, Fishbein E and Won Y-I 2014 Estimating sampling biases and measurement uncertainties of AIRS/AMSU-A temperature and water vapor observations using MERRA reanalysis *J. Geophys. Res. Atmos.* **119** 2725–41
- Huang B, Thorne P W, Banzon V F, Boyer T, Chepurin G, Lawrimore J H, Menne M J, Smith T M, Vose R S and Zhang H 2017 Extended reconstructed sea surface temperature, version 5 (ERSSTv5): upgrades, validations, and intercomparisons *J. Clim.* **30** 8179–205
- Hulley G and Hook S 2017 *MOD21A1D MODIS/Terra Land surface temperature/3-band emissivity daily L3 global 1 km SIN grid day V006* NASA EOSDIS Land Processes DAAC
- Ishihara K 2006 Calculation of global surface temperature anomalies with COBE-SST *Weather Service Bulletin* **73** S19–25
- IPCC 2013 *Climate Change 2013: The Physical Science Basis. Contribution of Working Group I to the Fifth Assessment Report of the Intergovernmental Panel on Climate Change* ed T Stocker (Cambridge and New York, NY: Cambridge University Press) p 1535
- Karl T R, Arguez A, Huang B, Lawrimore J H, McMahon J R, Menne M J, Peterson T C, Vose R S and Zhang H-M 2015 Possible artifacts of data biases in the recent global surface warming hiatus *Science* **348** 1469–72
- Keupp L, Pollinger F and Paeth H 2017 Assessment of future ENSO changes in a CMIP3/CMIP5 multi-model and multi-index framework *Int. J. Climatol.* **37** 3439–51
- McGrath D, Colgan W, Bayou N, Muto A and Steffen K 2013 Recent warming at summit, greenland: global context and implications *Geophys. Res. Lett.* **40** 2091–6

- Mears C A and Wentz F J 2017 A satellite-derived lower-tropospheric atmospheric temperature dataset using an optimized adjustment for diurnal effects *J. Clim.* **30** 7695–718
- Merchant C J *et al* 2013 The surface temperatures of Earth: steps towards integrated understanding of variability and change *Geosci. Instrum. Method. Data Syst.* **2** 305–21
- Merchant C J *et al* 2017 Uncertainty information in climate data records from Earth observation *Earth Syst. Sci. Data* **9** 511–27
- Morice C P, Kennedy J J, Rayner N A and Jones P D 2012 Quantifying uncertainties in global and regional temperature change using an ensemble of observational estimates: the HadCRUT4 data set *J. Geophys. Res., Atmos.* **117** D8
- NASA Public Affairs 2018 Long-term warming trend continued in 2017: NASA, NOAA <https://giss.nasa.gov/research/news/20180118/> (Accessed: 3 December 2018)
- Richardson M, Cowtan K, Hawkins E and Stolpe M B 2016 Reconciled climate response estimates from climate models and the energy budget of Earth *Nat. Clim. Change* **6** 931–5
- Rohde R, Muller R, Jacobsen R, Muller E, Perlmutter S, Rosenfeld A, Wurtele J, Groom D and Wickham C 2013 A new estimate of the average earth surface land temperature spanning 1753 to 2011 *Geoinform. Geostat.: Overview* **1** 1
- Sánchez-Lugo A, Morice C, Berrisford P and Argüez A 2018 Global surface temperatures *Bull. Amer. Meteor. Soc.* **99** S11–3
- Simmons A J, Berrisford P, Dee D P, Hersbach H, Hirahara S and Thépaut J-N 2016 A reassessment of temperature variations and trends from global reanalyses and monthly surface climatological datasets *Q. J. R. Meteorol. Soc.* **143** 101–19
- Sobrino J A, Sòria G and Prata A J 2004 Surface temperature retrieval from along track scanning radiometer 2 data: algorithms and validation *J. Geophys. Res.* **109** D11101
- Spencer R W, Christy J R and Braswell W D 2017 UAH Version 6 global satellite temperature products: methodology and results *Asia-Pac. J. Atmos. Sci.* **53** 121
- Susskind J, Barnett C and Blaisdell J 2003 Retrieval of atmospheric and surface parameters from AIRS/AMSU/HSB data in the presence of clouds *IEEE Trans. Geosci. Remote Sens.* **41** 390–409
- Susskind J, Barnett C, Blaisdell J, Iredell L, Keita F, Kouvaris L, Molnar G and Chahine M 2006 Accuracy of geophysical parameters derived from atmospheric infrared sounder/advanced microwave sounding unit as a function of fractional cloud cover *J. Geophys. Res.* **111** D09S17
- Susskind J, Blaisdell J and Iredell L 2014 Improved methodology for surface and atmospheric soundings, error estimates, and quality control procedures: the AIRS science team version-6 retrieval algorithm *J. Appl. Remote Sens.* **8** 084994
- Susskind J, Blaisdell J M, Iredell L and Keita F 2011 Improved temperature sounding and quality control methodology using AIRS/AMSU data: the AIRS science team version 5 retrieval algorithm *IEEE Trans. Geosci. Remote Sens.* **49** 0196–2892
- Veal K L, Corlett G K, Ghent D, Llewellyn-Jones D T and Remedios J J 2013 A time series of mean global skin SST anomaly using data from ATSR-2 and AATSR *Remote Sens. Environ.* **135** 64–76
- Vose R S *et al* 2012 NOAA's merged land-ocean surface temperature analysis *Bull. Am. Meteorol. Soc.* **93** 1677–85
- Way R G, Oliva F and Viau A E 2017 Underestimated warming of northern Canada in the Berkeley Earth temperature product *Int. J. Climatol.* **37** 1746–57